

Photodynamics of All-*trans* Retinal Protonated Schiff Base in Bacteriorhodopsin and Methanol Solution

Xin Li, Lung Wa Chung,* and Keiji Morokuma*

Fukui Institute for Fundamental Chemistry, Kyoto University, Kyoto 606-8103, Japan

S Supporting Information

ABSTRACT: Nonadiabatic ONIOM(CASSCF:AMBER) and CASSCF simulations elucidated different photodynamics of an all-*trans* retinal protonated Schiff base (RPSB) in bacteriorhodopsin and methanol as well as without an environment. The bR protein matrix holds RPSB tight via specific interactions and promotes bond-specific (along the C13=C14 bond), unidirectional, and ultrafast photoisomerization with a high quantum yield. In contrast, in methanol and for the twisted bare RPSB, photoisomerization is not bond-specific (mainly along the C11=C12 bond), is nonunidirectional, and is ineffective. Therefore, bR efficiently “catalyzes” photoisomerization and stores enough energy to promote the subsequent proton pumping and protein conformational changes.

Bacteriorhodopsin (bR) is a transmembrane protein in the purple membrane of *Halobacterium salinarum*.¹ An all-*trans* retinal protonated Schiff base (RPSB) is covalently linked to the Lys216 of the protein in the light-adapted bR. Absorption of a photon by RPSB can trigger a photocycle with several photostationary states (Scheme 1). The first step of this photocycle is photoisomerization of all-*trans* RPSB to give the 13-*cis* form in an ultrafast and efficient manner (quantum yield: ~ 0.6 – 0.7),² which prompts vectorial proton transfer and protein conformational changes. Transient spectroscopic studies showed that, after photoexcitation in the Franck–Condon (FC) region, photoisomerization of RPSB was observed to rapidly give a twisted configuration in S_1 (>200 fs).³

In comparison, in a homogeneous methanol solution, photoisomerization of RPSB is slower, nonspecific, and inefficient, to give a mixture of different isomers, the 9-*cis* (0.02), 11-*cis* (0.14), and 13-*cis* (0.01) forms.⁴ Also, the reaction time of photoisomerization is much slower in solutions (on the picosecond time scale).⁵ The different reaction mechanisms and photodynamics of RPSB in bR and solutions are of great importance but still remain unclear. In this study, we report nonadiabatic (NA) ONIOM(CASSCF:AMBER) and CASSCF molecular dynamics (MD) simulations (mainly on S_1 and S_0 surfaces) to elucidate the effects of different environments on the photodynamics of RPSB. To our knowledge, it is the first NA CASSCF/AMBER MD simulation including all π bonds of RPSB as the QM part in bR as well as the first comparison of photodynamics in bR and in methanol.⁶

ONIOM(B3LYP/6-31G:AMBER) MD simulations with an electronic embedding (EE) scheme was performed to equilibrate the systems and then sample ground-state structures at 298 K. Afterward, ONIOM(CASSCF(12e,12o)/6-31G:AMBER) MD simulations in the constant energy ensemble were carried out. For the simulations in bR and methanol, around FC and fluorescent state regions, the ONIOM(CASSCF:AMBER)-EE method gives a wrong order of the covalent A_g -like excited state (S_2) and ionic B_u -like excited state (S_1).⁶ⁿ This problem can be remedied by using the computationally unaffordable MS-CASPT2 or MRCI method. To remedy this unrealistic situation, the mechanical embedding (ME) scheme was first used, and then the EE scheme was adopted when $\Delta E_{S_1-S_0} < \sim 35$ kcal/mol.

As shown in Tables S1 and S3 (Supporting Information), time to access the crossing region is similar, when either we used the ONIOM-ME method only in S_1 or we switched to use the ONIOM-EE method. Therefore, the overall qualitative conclusions should not be affected by switching to the ONIOM-EE method.^{7a}

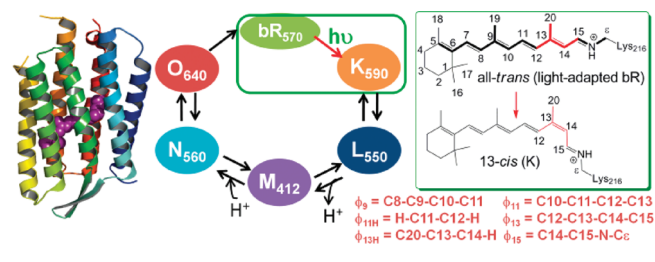
In bR, as shown in Figures 1a,c and S1 (Supporting Information) and Table 1, photoexcited RPSB underwent ultrafast radiationless decay ($S_1 \rightarrow S_0$) exclusively via a torsional change along ϕ_{13} (Scheme 1). The mean excited-state (S_1) lifetime is about 114–162 fs (ranging from 75 to 334 fs) via nonadiabatic crossing (NC) and crossing seam (CS),^{7b} which is shorter than the experimental values (>200 fs).³ It is partly attributed to the over-repulsive potential of the CASSCF method.⁸ Photoisomerization giving the 13-*cis* form is very efficient with a quantum yield (Φ_{photoiso}) of 0.69–0.86, which is in good agreement with the experiments (~ 0.6 – 0.7).² Moreover, photoisomerization in bR is always unidirectional (increasing ϕ_{13} , see also Figure S2, Supporting Information).

Additional CASSCF MD simulations for bare RPSB, with the same initial conditions but removing the protein matrix, were further performed. Notably, the equilibrium structure of RPSB in bR in S_0 is slightly twisted at ϕ_{13} (X-ray and ONIOM-optimized ones: $\phi_{13} = 203^\circ$).⁹ Although the chromophore is pretwisted, the unidirectional and bond-specific photoisomerization is lost in the absence of the protein matrix. The rotations can take place in both directions (Figure S4, Supporting Information) and along the following torsions: ϕ_9 (6.25%), $\phi_9 + \phi_{11}$ (6.25%), ϕ_{11} (56.25%), and ϕ_{13} (31.25%). Also, compared to bR, this twisted bare retinal model takes a longer time to access the crossing region (Table S1, Supporting Information). Therefore, the protein matrix is vital to efficiently channelling RPSB to the unique rotation (intramolecular vibrational redistribution) during the photoisomerization process. Comparatively, the protein matrix in rhodopsin (Rh) is not critical for the photoisomerization of the 11-*cis* retinal, which is partly driven by a steric repulsion between the C10–H and C13–Me moieties of the 11-*cis* retinal.^{6ln}

Received: August 8, 2011

Published: August 09, 2011

Scheme 1. bR Protein, Key Events in the Photocycle, Retinal Protonated Schiff Base (QM Part in Bold), and Definition of the Key Torsions



The bond-specific and unidirectional photoisomerization in bR is controlled by stereospecific chromophore–protein interactions. Namely, nearby residues (Trp86, Thr90, Met118, Ile119, Trp182, and Tyr185) sandwich RPSB except the C14C15N part (Figure 2a). Therefore, rotations around other bonds are suppressed by these residues, and the protein matrix specifically facilitates the rotation around the C13=C14 bond in a small preset cavity. The C14HC15-HNH part has the largest displacement at the crossings relative to the FC structure (Figure 2b). In contrast, photoisomerization of all-*trans* RPSB in bathorhodopsin (bathoRh) leads to the 11-*cis* form, presumably due to a lack of steric hindrance around the C11=C12 bond (Figure S5, Supporting Information).¹⁰ In addition, C14H of RPSB in bR is in close contact with Trp86 (Figure 2a), which results in a pretwisted C13=C14 bond in S_0 . Thus, photoisomerization occurs only toward one direction to avoid the repulsion with Trp86.^{6b,c} It should be noted that the active sites of other microbial rhodopsin homologues (e.g., SRII and HR) are similar to bR (Figure S6, Supporting Information). We believe microbial rhodopsins may use a similar mechanism to control photoisomerization.

In methanol (compared to bR), the nearly planar RPSB takes a longer time to decay via one of three torsional changes: ϕ_9 , ϕ_{11} , or ϕ_{13} (Scheme 1, Table 1, Figures 1b,c and S1, S3, and S7, Supporting Information). The mean S_1 lifetime is about 748 and 817 fs (ranging from 208 to 2488 fs) via NC or CS,^{7b} respectively. Also, Φ_{photoiso} giving the 11-*cis* form is about 0.11 for NC, while that leading to the 11-*cis*, 9,11-di-*cis*, and 13-*cis* forms is 0.33, 0.07, and 0.07 for CS, respectively. It is qualitatively consistent with a smaller observed Φ_{photoiso} .⁴ Moreover, the rotation is not unidirectional in methanol (Figure 1b). Also, displacements of RPSB and nearby methanol molecules are larger at the crossing (Figure 2c), due to a more flexible solution cavity. Thus, solvent reorganization and a lack of the pretwisted RPSB (reactant destabilization) should increase the S_1 lifetime.

For most cases in bR, the twisting along ϕ_{13} and ϕ_{15} takes place in the opposite directions (Figure 3a). At the $S_1 \rightarrow S_0$ crossings, the former motion (average: $\sim +61^\circ$) is more profound than the latter ($\sim -32^\circ$; Figures 1a and S2, S8, and S9, Supporting Information). These large torsional motions come mainly from motions of the C14H–C15H part, in particular, hydrogen atoms due to their lowest mass and size. Once the twisted system in S_1 makes the transition to S_0 and gives the 13-*cis* photoproduct, ϕ_{15} generally continues to twist until a maximum is reached and then turns back to the *trans* position (Figure 3a). Such an asynchronous crankshaft motion,^{6h,i,k} which allows the rotation of the C13–C14–C15–N moiety in the limited protein cavity (Figures S8–S9, Supporting Information), is the main space-saving decay pathway in bR.

In methanol, torsions along ϕ_9 (average: $\sim +36^\circ$) and ϕ_{11} ($\sim -74^\circ$) bonds are mostly twisted in the opposite directions at

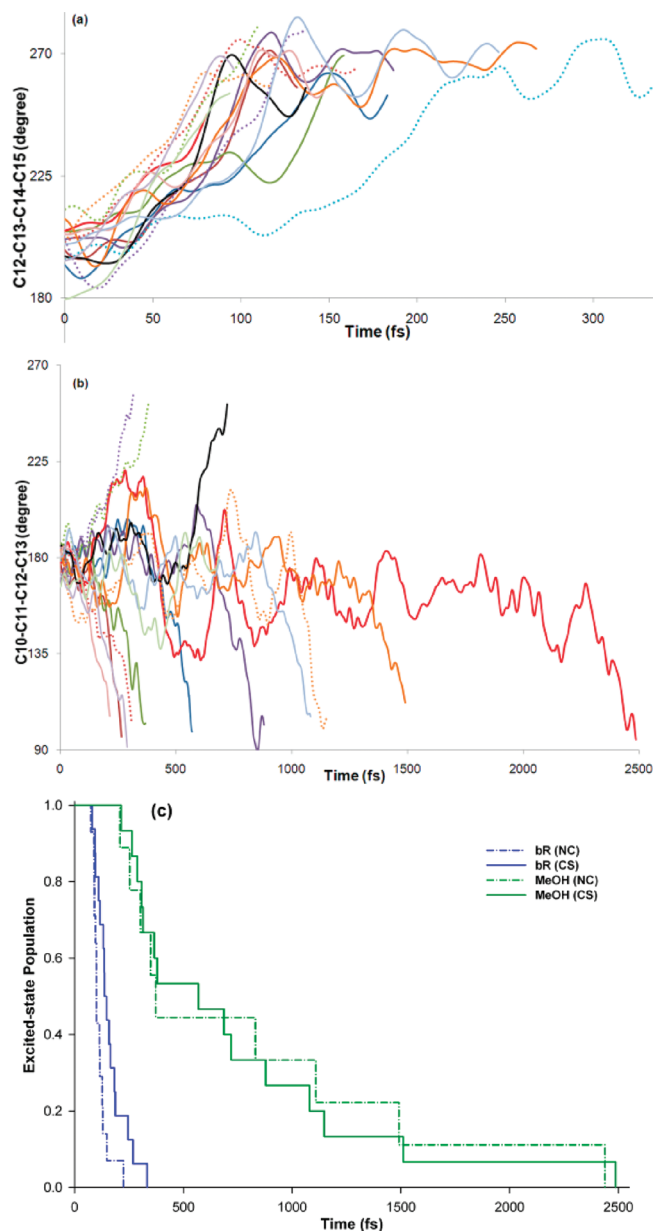


Figure 1. Changes of the rotating dihedral in S_1 until CS (ref 7b): (a) ϕ_{13} in bR and (b) ϕ_{11} in methanol (also see Figure S3, Supporting Information). (c) Excited-state population for photoisomerization in bR and methanol.

Table 1. The Mean S_1 Lifetime τ (fs) and Quantum Yield Φ_{photoiso} (Photoproducts) for Photoisomerization in bR and Methanol

| | τ_{NC}^a | $\Phi_{\text{photoiso,NC}}^b$ | τ_{CS}^c | $\Phi_{\text{photoiso,CS}}^b$ |
|----------|----------------------|-------------------------------|----------------------|-------------------------------|
| bR | 114 | 0.86(13C) | 162 | 0.69(13C) |
| Methanol | 817 | 0.11(11C) | 748 | 0.33(11C) ^d |

^a Nonadiabatic crossing (ref 7b). ^b 13-*cis* (13C) and 11-*cis* (11C) forms.

^c Crossing seam (ref 7b). ^d The formation of one 9,11-di-*cis* form and one 13-*cis* form was observed.

the $S_1 \rightarrow S_0$ crossings (Figures 1b and S3, S8, and S9, Supporting Information). The twisting along ϕ_{13} ($\sim +18^\circ$) is much smaller, except one case that led to the 13-*cis* form. Moreover, from the

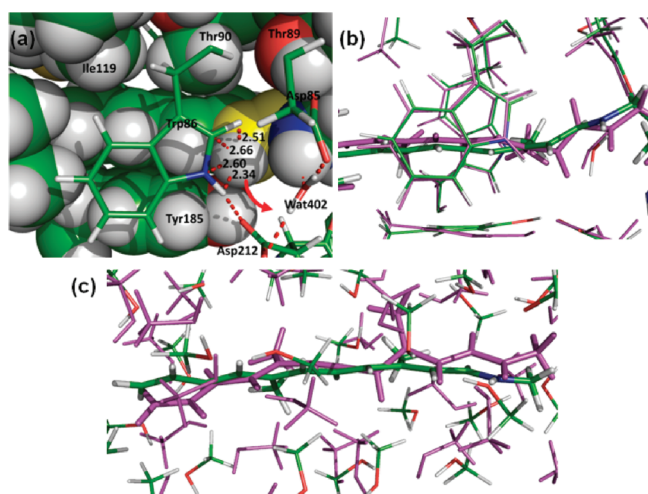


Figure 2. (a) ONIOM-optimized active-site structure of bR. The C14 and C15 are highlighted by a yellow color, and the close contacts between HC14 and Trp86 are given in Ångströms. Superimposition of FC (green) and crossing (pink) structures in (b) bR and (c) methanol.

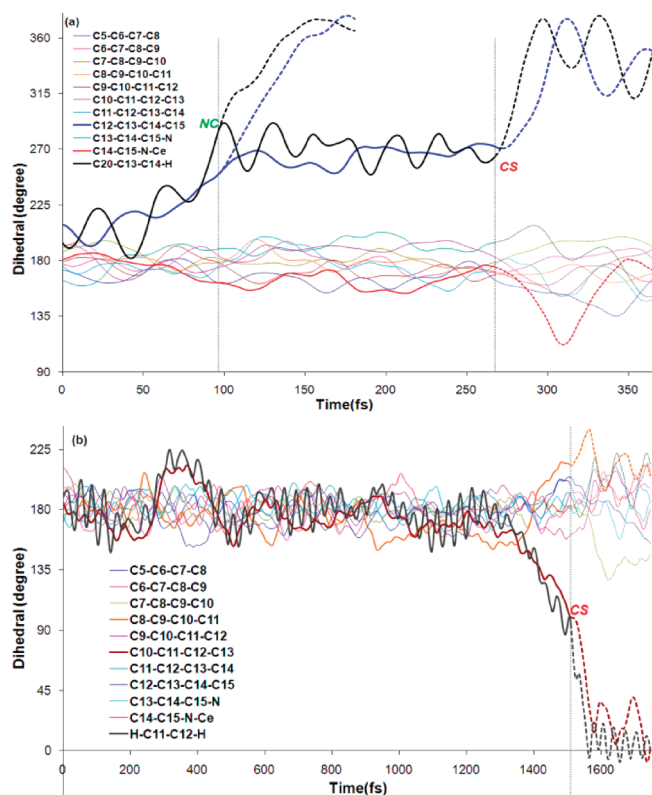


Figure 3. An example of the evolution of dihedrals for photoisomerizations of (a) all-*trans*→13-*cis* in bR and (b) all-*trans*→11-*cis* in a methanol solution.

twisted form in S_1 to the 11-*cis* photoproduct in S_0 , ϕ_9 continues to twist to a maximum and then turns back (Figure 3b).¹¹ Again, the crankshaft motion is the main pathway for the decay in methanol. Overall, the crankshaft motion is the major pathway for the decay and photoisomerization of RPSB in bR, Rh, methanol, and the gas phase^{6h,k-n} and could also operate in the other retinal proteins or solutions, although rotations at different angles/bonds can be involved.

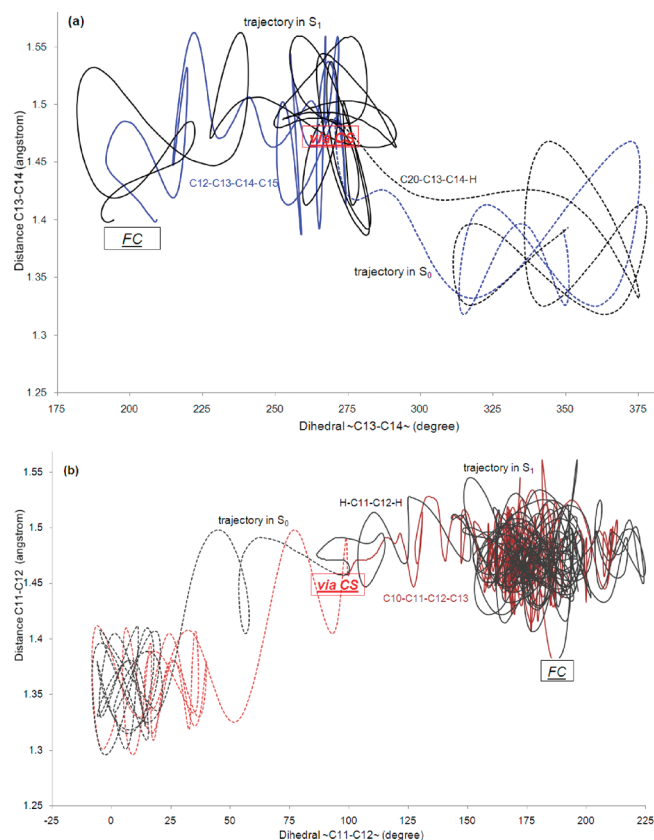
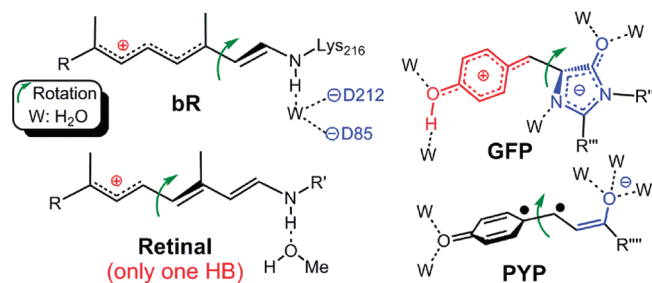


Figure 4. Dynamic changes of rotating torsions versus the bond length for photoisomerizations of (a) all-*trans*→13-*cis* in bR and (b) all-*trans*→11-*cis* in a methanol solution.

At all S_1 – S_0 crossings, the largest twist involves hydrogen atoms, i.e., ϕ_{13H} (average: $\sim 81^\circ$) in bR and ϕ_{11H} ($\sim 88^\circ$) in methanol (Scheme 1 and Figure S8, Supporting Information). A hydrogen-out-of-plane (HOOP) mode, the difference between ϕ_{13H} and ϕ_{13} torsions in bR or between ϕ_{11H} and ϕ_{11} torsions in methanol, oscillates around zero in S_1 (Figure S10, Supporting Information), indicating a small pyramidalization at these carbons. Pyramidalization, however, becomes important in some crossing regions, especially in bR.^{6c} Just after the S_1 → S_0 transition, ϕ_{13H} and ϕ_{11H} torsions generally move most rapidly (Figure S11, Supporting Information), due to the light-mass hydrogen atom. Interestingly, the larger and faster ϕ_{13H} torsional change can control the stereochemistry of the photoproduct.^{6h,k} In comparison, a large-amplitude oscillation of the HOOP mode was found in the whole photoisomerization of highly twisted RPSB in bathoRh.^{6h} The faster dynamics of torsions with hydrogen atom(s) was also observed in Dronpa and rhodopsin (Rh)^{6h,12} and may operate in other photoisomerization systems.

Photoisomerization of RPSB generally follows a two-state, two-mode mechanism (Figure 4). However, an A_g -like (S_2) state occasionally mixes with the B_u -like S_1 state just after photoexcitation,¹³ where $\Delta E_{S_2-S_1}$ (MS-CASPT2:MM-EE) is small (~ 1 – 8 kcal/mol), due to electrostatic and polarization interaction of the QM part with the protein and solvent (Figure S12, Supporting Information). This has been found in a few trajectories in bR and methanol. Before reaching the S_1 → S_0 crossing, $\Delta E_{S_2-S_1}$ oscillates around ~ 20 kcal/mol, and the oscillation strength for S_1 → S_2 is non-negligible. This is consistent with the

Scheme 2. Schematic Hydrogen Bonds (HB) of the Twisted Structures for bR, Retinal (In Methanol), GFP, and PYP Chromophores



recently observed near-IR absorption.^{5b} At the $S_1 \rightarrow S_0$ crossings in bR, large electrostatic and polarization interactions with the protein, mainly from Asp85 and Asp212,¹⁴ can help reduce the energy gap by ~ 16 kcal/mol; this interaction is much smaller ($\sim 2\text{--}3$ kcal/mol) in methanol.

Hydrogen bonding between the NH of RPSB and its nearby water molecule w402 in bR is weakened in the $S_1 \rightarrow S_0$ crossing region and is furthermore reduced during the *trans-cis* isomerization in S_0 (Figures 2a and S13, Supporting Information), due to translocation of the positive charge of RPSB and w402 being tightly held by Asp85 and Asp212. Notably, such a weaker hydrogen bond partly contributes to energy storage.^{6d} However, in methanol solution, hydrogen bonding between RPSB and the nearby methanol molecule is not necessarily weakened during the *trans-cis* photoisomerization. In some trajectories, when the methanol molecule loses the hydrogen bond with RPSB, another (or two) nearby methanol molecule(s) can come and form new hydrogen bond(s) with RPSB (Figure S14, Supporting Information). Interestingly, multiple hydrogen bonds were suggested to promote the decay of GFP and PYP chromophores in water by preferentially stabilizing S_1 at the crossings (Scheme 2).^{12,15} The weaker solvent effect at the crossings for RPSB in methanol is partly attributed to the existence of only one hydrogen bond with RPSB (Scheme 2).

In summary, our simulation has shown that the bR protein matrix is essential for catalyzing bond-specific, unidirectional, and efficient photoisomerization of RPSB. The protein environments specifically hold the chromophore tight for the controlled reaction. Bond specificity, unidirectionality, and efficiency are all lost for RPSB in methanol or for the twisted bare RPSB. The two-state, two-mode mechanism generally operates in bR and methanol, but an A_g -like state can occasionally mix with the B_u -like state in S_1 just after photoexcitation. Transition from S_1 to close-lying S_2 may account for the recently observed near-IR absorption in solution.^{5b} The crankshaft motion is the dominant pathway that leads to internal conversion and isomerization ($S_1 \rightarrow S_0$). The hydrogen bond between RPSB and the nearby water molecule is weakened during the photoisomerization process in bR, but it is not necessarily weakened in methanol. Furthermore, at the crossings, there are strong electrostatic and polarization interactions on RPSB by the protein, but this is much smaller in methanol. These features tailored for bR are vital to efficiently converting the solar energy to drive proton transfer and protein conformational changes.

■ ASSOCIATED CONTENT

S Supporting Information. Computational details, Figures S1–S15, Tables S1–S3, and Movies S1–S2. This material is available free of charge via the Internet at <http://pubs.acs.org>.

■ AUTHOR INFORMATION

Corresponding Author

*E-mail: morokuma@fukui.kyoto-u.ac.jp; chung@fukui.kyoto-u.ac.jp.

■ ACKNOWLEDGMENT

L.W.C. acknowledges FIFC Fellowship. This work is in part supported by Japan Science and Technology Agency with a Core Research for Evolutional Science and Technology grant in the Area of High Performance Computing for Multiscale and Multiphysics. Calculations in part at Research Center of Computer Science (Institute for Molecular Science) and Academic Center for Computing and Media Studies (Kyoto University) are also acknowledged.

■ REFERENCES

- (1) Oesterhelt, D.; Stoebenius, W. *Nat. New Biol.* **1971**, 233, 149–152.
- (2) (a) Govindjee, R.; Balashov, S. P.; Ebrey, T. G. *Biophys. J.* **1990**, 58, 597–608. (b) Tittor, J.; Oesterhelt, D. *FEBS Lett.* **1990**, 263, 269–273.
- (3) (a) Mathies, R. A.; Cruz, C. H. B.; Pollard, W. T.; Shank, C. V. *Science* **1988**, 240, 777–779. (b) Gai, F.; Hasson, K. C.; McDonald, J. C.; Anfinrud, P. A. *Science* **1998**, 279, 1886–1891. (c) Kobayashi, T.; Saito, T.; Ohtani, H. *Nature* **2001**, 414, 531–534. (d) Herbst, J.; Heyne, K.; Diller, R. *Science* **2002**, 297, 822–825. (e) Schenkl, S.; van Mourik, F.; van der Zwan, G.; Haacke, S.; Chergui, M. *Science* **2005**, 309, 917–921. (f) Shim, S.; Dasgupta, J.; Mathies, R. A. *J. Am. Chem. Soc.* **2009**, 131, 7592–7597.
- (4) Koyama, Y.; Kubo, K.; Komori, M.; Yasuda, H.; Mukai, Y. *Photochem. Photobiol.* **1991**, 54, 433–443.
- (5) (a) Logunov, S. L.; Song, L.; El-Sayed, M. J. *Phys. Chem.* **1996**, 100, 18586–18591. (b) Loevsky, B.; Wand, A.; Bismuth, O.; Friedman, N.; Sheves, M.; Ruhman, S. *J. Am. Chem. Soc.* **2011**, 133, 1626–1629.
- (6) (a) Humphrey, W.; Lu, H.; Logunov, I.; Werner, H. J.; Schulten, K. *Biophys. J.* **1998**, 75, 1689–1699. (b) Tajkhorshid, E.; Baudry, J.; Schulten, K.; Suhai, S. *Biophys. J.* **2000**, 78, 683–693. (c) Hayashi, S.; Tajkhorshid, E.; Schulten, K. *Biophys. J.* **2003**, 85, 1440–1449. (d) Hayashi, S.; Tajkhorshid, E.; Kandori, H.; Schulten, K. *J. Am. Chem. Soc.* **2004**, 126, 10516–10517. (e) Altoè, P.; Cembran, A.; Olivucci, M.; Garavelli, M. *Proc. Natl. Acad. Sci. U.S.A.* **2010**, 107, 20172–20177. (f) Szymczak, J. J.; Barbatti, M.; Lischka, H. *J. Phys. Chem. A* **2009**, 113, 11907–11918. (g) Phatak, P.; Ghosh, N.; Yu, H.; Cui, Q.; Elstner, M. *Proc. Natl. Acad. Sci. U.S.A.* **2008**, 105, 19672–19677. (h) Schapiro, I.; Ryazantsev, M. N.; Frutos, L. M.; Ferré, N.; Lindh, N.; Olivucci, M. *J. Am. Chem. Soc.* **2011**, 133, 3354–3364. (i) Warshel, A. *Nature* **1976**, 260, 679–683. (j) Warshel, A.; Chu, Z. T. *J. Phys. Chem. B* **2001**, 105, 9857–9871. (k) Polli, D.; Altoè, P.; Weingart, O.; Spillane, K. M.; Manzoni, C.; Brida, D.; Tomasello, G.; Orlandi, G.; Kukura, P.; Mathies, R. A.; Garavelli, M.; Cerullo, G. *Nature* **2010**, 467, 440–443. (l) Weingart, O. *J. Am. Chem. Soc.* **2007**, 129, 10618–10619. (m) Ishida, T.; Nanbu, S.; Nakamura, H. *J. Phys. Chem. A* **2009**, 113, 4356–4366. (n) Hayashi, S.; Tajkhorshid, E.; Schulten, K. *Biophys. J.* **2009**, 96, 403–416 and references therein.
- (7) (a) Detailed descriptions of the method and program citations are in the Supporting Information (SI). (b) Transition probability for NC and CS is >0.5 and assumed to be 1.0, respectively. See detailed definitions in the SI.
- (8) Valsson, O.; Filippi, C. *J. Chem. Theory Comput.* **2010**, 6, 1275–1292.
- (9) Luecke, H.; Schobert, B.; Richter, H.-T.; Cartailier, J.-P.; Lanyi, J. K. *J. Mol. Biol.* **1999**, 291, 899–911.

- (10) (a) Spalink, J. D.; Reynolds, A. H.; Rentzepis, P. M.; Sperling, W.; Applebury, M. L. *Proc. Natl. Acad. Sci. U.S.A.* **1983**, *80*, 1887–1891. (b) Nakamichi, H.; Okada, T. *Angew. Chem., Int. Ed.* **2006**, *45*, 4270–4273.
- (11) Torsional changes around terminal single bonds (e.g., C6–C7 and/or C8–C9) of vibrationally hot RPSB were large in S_0 in methanol, but they are suppressed by the protein.
- (12) Li, X.; Chung, L. W.; Mizuno, H.; Miyawaki, A.; Morokuma, K. *J. Phys. Chem. Lett.* **2010**, *1*, 3328–3333.
- (13) Three-state model: Hasson, K. C.; Gai, F.; Anfinrud, P. A. *Proc. Natl. Acad. Sci. U.S.A.* **1996**, *93*, 15124–15129 and refs 5b and 6a.
- (14) Song, L.; El-Sayed, M. A.; Lanyi, J. K. *Science* **1993**, *261*, 891–894.
- (15) (a) Boggio-Pasqua, M.; Robb, M. A.; Groenhof, G. *J. Am. Chem. Soc.* **2009**, *131*, 13580–13581. (b) Virshup, A. M.; Punwong, C.; Pogorelov, T. V.; Lindquist, B. A.; Ko, C.; Martínez, T. J. *J. Phys. Chem. B* **2009**, *113*, 3280–3291 and references therein.